Available online at www.sciencedirect.com
SCIENCE DIRECT®
Engineering Structures 27 (2005) 951–962
ENGINEERING STRUCTURES
www.elsevier.com/locate/engstruct

Seismic behaviors of columns in ordinary and intermediate moment resisting concrete frames

Sang Whan Han*, N.Y. Jee

Department of Architectural Engineering, Hanyang University, Seoul 133-791, Republic of Korea

Received 30 March 2004; received in revised form 31 January 2005; accepted 31 January 2005
Available online 10 March 2005

Abstract

The objective of this study was to investigate the seismic behaviors of columns in Ordinary Moment Resisting Concrete Frames (OMRCF) and Intermediate Moment Resisting Concrete Frames (IMRCF). For this purpose, two three-story OMRCF and IMRCF were designed according to the minimum design and reinforcement detailing requirements specified in ACI 318-02. This study assumed that the building was located in seismic zone 1, as classified by UBC. According to ACI 318-02 the reinforcement detailing requirements for OMRCF are less stringent than those for either IMRCF or SMRCF (Special Moment Resisting Concrete Frames). Tests were carried out to evaluate the seismic behaviors of OMRCF and IMRCF columns using 2/3 scale model columns. Each column was considered as consisting of an upper part and lower part divided at the point of inflection. Quasi-static reversed cyclic loading was applied to the specimens with either constant or varying axial forces. The test variables of this experimental study were the type of axial force (constant and varying, and low and high), the existence of lap splices (with or without lap splice) and type of moment resisting concrete frame (OMRCF or IMRCF). It was observed that all OMRCF and IMRCF column specimens had strength larger than that required by ACI 318, and they had drift capacities greater than 3.0% and 4.5%, respectively. However, the drift capacity of specimens varied with respect to the existence of lap splices and the spacing of lateral reinforcement at column ends.

Keywords: Seismic behavior; Columns; Reinforcement details; Seismic design

1. Introduction

Moment frames have been widely used for seismic resisting systems due to their superior deformation and energy dissipation capacities. A moment frame consists of beams and columns, which are rigidly connected. The components of a moment frame should resist both gravity and lateral load. Lateral forces are distributed according to the flexural rigidity of each component. ACI 318-02 [1] states the design and reinforcement detailing requirements for each type of moment frame and each earthquake risk level. The type of moment frame should be selected according to levels of seismic risk or seismic design category. Seismic risk levels can be classified into low, moderate and high according to seismic zones specified in UBC [2]. Seismic design category is specified in NHERP [3] and IBC [8].

ACI 318-02 classifies concrete moment frames into three types: Ordinary Moment Resisting Concrete Frame (OMRCF); Intermediate Moment Resisting Concrete Frame (IMRCF); and Special Moment Resisting Concrete Frame (SMRCF). Fig. 1 shows the minimum column reinforcement details for the columns of OMRCF, IMRCF, and SMRCF specified in ACI 318 and notes [1,4].

OMRCF and IMRCF are the most popular types of moment frames in low to moderate seismic zones. The design and reinforcement requirements for OMRCF and IMRCF are less stringent than those for SMRCF. When a large earthquake occurs, SMRCF is expected to have superior ductility and provide superior energy dissipation capacity. In current seismic design procedures, design base

* Corresponding author. Tel.: +82 2 2290 1715; fax: +82 2 2291 1716.
E-mail address: swhan@hanyang.ac.kr (S.W. Han).

0141-0296/$ - see front matter © 2005 Elsevier Ltd. All rights reserved.
doi:10.1016/j.engstruct.2005.01.012

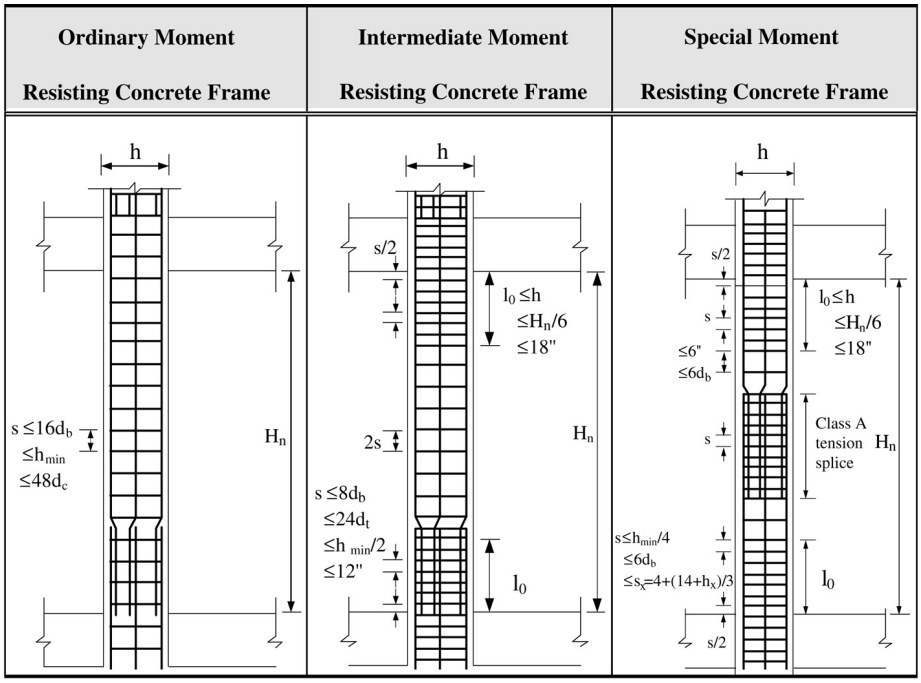

d_b, d_t: diameter of longitudinal and transverse bars, s: spacing of lateral bars, h_{min}: minimum dimension of column, s_x :longitudinal spacing of transverse bars within l_o

Fig. 1. Minimum reinforcement details for columns.

Notation

A_g	gross area of column
f'_c	specified compressive strength of concrete
f_y	specified yield strength of nonprestressed reinforcement
M_{max}	maximum moment resistance of the specimen
M_{ACI}	moment capacity calculated using ACI 318-99 procedures
V_{ACI}	nominal shear strength according to ACI 318-99
Δ_{max}	maximum displacement
θ_{max}	maximum drift angle

shear force shall be calculated by elastic strength demand divided by R factor (≥ 1). R factor accounts for ductility, overstrength, redundancy, and damping inherent in a structural system. Current design provisions assigned the highest R factor to SMRCF, and the lowest R factor to OMRCF because of its less stringent design requirement. It should be noted that design base shear becomes larger with decreasing R factor.

This study focused on the behaviors of first story columns in moment resisting frames. For this purpose, three-story OMRCF and IMRCF buildings were designed according to ACI 318-02. Experimental test of columns in the first story of those buildings was carried out to investigate the seismic behavior of the columns. This study considered that a column consisted of an upper part and lower part divided at the point of inflection.

Eight 2/3 scale column specimens ($2 \times 2 \times 2 = 8$) representing the lower and upper part (2) of the exterior and interior columns (2) in the OMRCF and IMRCF (2) were made. Lower column specimens had lap splices whereas upper column specimens had continuous longitudinal reinforcement. The most significant difference in OMRCF and IMRCF columns is the spacing of the transverse reinforcement at the end of the column. Quasi-static reversed cyclic loading was applied to the specimens with either fixed or varying axial forces.

The test variables in this study were type of axial force (constant and varying, and low and high), existence of lap splices (with or without lap splice) and type of moment resisting concrete frames (OMRCF or IMRCF).

2. Previous studies

Han et al. [6,7] have evaluated the seismic performance of a three-story OMRCF. In their studies maximum lateral force was measured during the test and compared with the design base shear force specified in current codes. Moreover, this study carried out seismic performance evaluation of the three-story OMRCF using a capacity spectrum method.

Lee and Woo [9] investigated the seismic performance of low-rise reinforced concrete (RC) frames with non-seismic detailing. They considered a bare frame and a masonry infilled frame. An experiment was conducted

using 1/5 scaled specimens having two bays and three stories. They found that RC moment frames had a certain seismic resistance even though they were designed without considering seismic loads. Furthermore, masonry infill was beneficial to the seismic performance of the frame.

Aycardi et al. [10] investigated the behavior of gravity load-designed reinforced concrete column members under simulated seismic loading. They tested four column specimens governed by flexure under reversed cyclic loading at increasing drift amplitudes. It was observed that all column specimens were capable of sustaining at least two cycles of loading at a 4% drift angle.

Lynn et al. [11] tested eight reinforced concrete column specimens having typical details of those built before the mid-1970s. This study observed that column specimens that were governed by shear experienced gravity load failure soon after loss of lateral force resistance. When flexure was dominant in specimens, gravity load capacity was maintained to large displacement.

3. Experimental program

3.1. Design of building frames

Typical three-story office buildings were designed. Seismic resistance for these buildings was provided by OMRCF and IMRCF. The dimension and design loads were adopted from Han [6]. Fig. 2 shows the dimensions of the building.

Specified compressive strength (f_c') of concrete was assumed to be 23.5 MPa. Longitudinal reinforcement and reinforcement for hoop and stirrup were assumed to have a yield strength (f_y) of 392.3 MPa. Design loads for a typical office building were used (5.2 kPa for dead load and 2.4 kPa for live load). The section of all columns and beams in the model frames were assumed to be 330 mm × 330 mm and 250 mm × 500 mm, respectively.

The buildings were assumed to be located in seismic zone 1 as classified in UBC [2]. Member forces were obtained using SAP 2000 (2000). Gravity loads governed the member design. Since the seismic load was small, OMRCF and IMRCF had the same member sizes as well as the same amount of reinforcement except for the transverse reinforcement in columns and beams (see Fig. 3). This design was desirable for this study since this study attempted to investigate the effect of different reinforcement details of OMRCF and IMRCF columns on seismic behaviors of those columns without interference of other factors such as amount of longitudinal reinforcement and different member sizes.

3.2. Column specimens

As shown in Fig. 2, only the columns in the first story were evaluated since these columns should resist the largest axial and lateral forces during an earthquake. The exterior

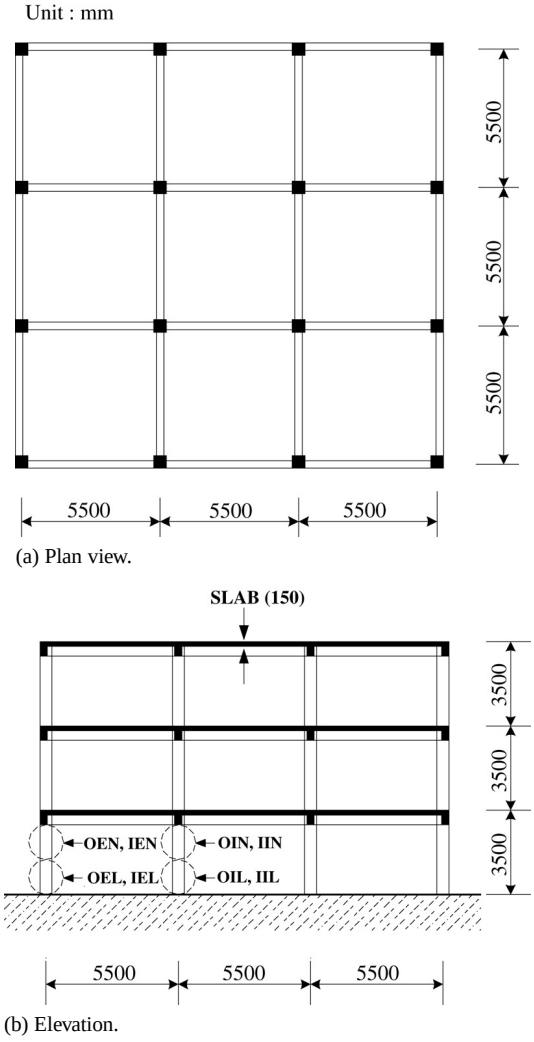

Fig. 2. Building layouts.

columns in the first story of the two model frames were designed for an axial force of 644.3 kN and a bending moment of 37 kN m, and the interior columns were designed for an axial load of 1234.7 kN and a bending moment of 47.1 kN m. It is noted that those design forces contain load factors.

All columns had a section of 330 mm × 330 mm and contained four longitudinal reinforcements (D19 (19.1 mm diameter), f_y = 392.3 MPa). Column longitudinal reinforcement ratio (ρ) was 1.01%, which slightly exceeded a minimum longitudinal reinforcing steel of 1.0% (Section 10.9.1 in ACI 318-02).

Maximum shear force in the first story columns induced by factored gravity loads was 31.4 kN. According to the formula in Section 11.3.1.2 of the ACI 318-02, the concrete shear strength of the first story columns (V_c) was calculated as 73.5 kN. Minimum tie reinforcement (D10 with a diameter of 9.53 mm) with spacing of 300 mm was placed throughout the column in the OMRCF (Section 7.10.5.2 in ACI 318-02) and the first tie reinforcement was placed 150 mm from the slab or footing surface according

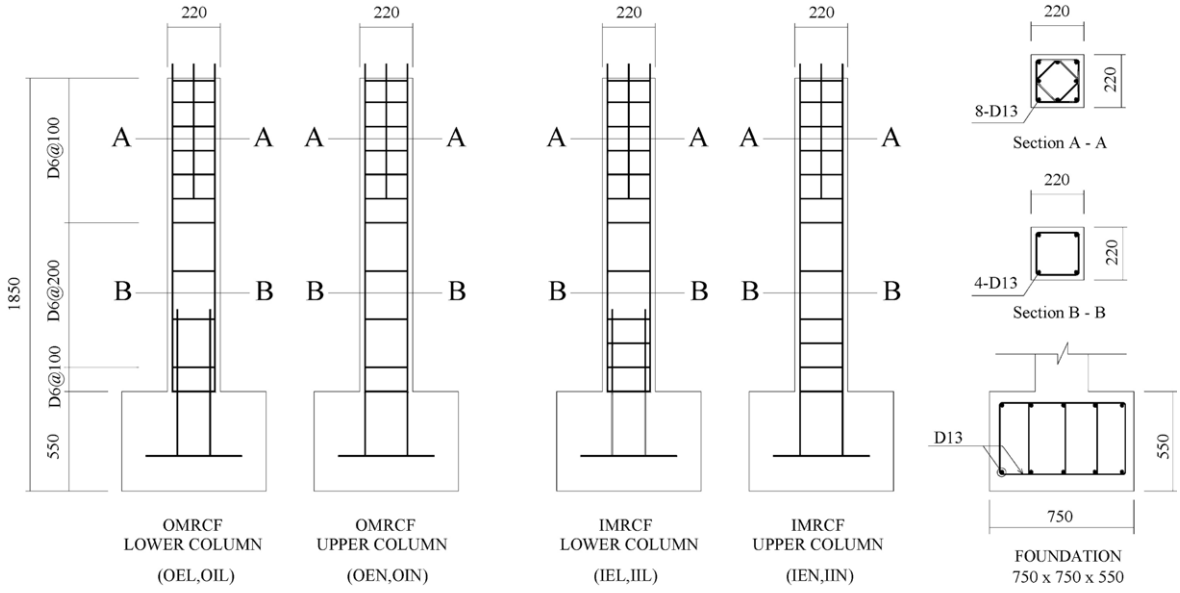

Fig. 3. Column specimens.

to the requirement of the first tie location specified in Section 7.10.5.4 in ACI 318-02.

Fig. 3 shows that the first tie was placed 100 mm from the slab in 2/3 scale specimens. The longitudinal reinforcement details in the IMRCF columns and the OMRCF columns were exactly the same. Tie spacing in the plastic hinging region of the IMRCF columns, however, was half of the tie spacing in the OMRCF columns. The yield strength of D10 was 392.3 MPa. A lap splice length of 525 mm was required for tension according to Section 12.15 in ACI 318-02. Lap splices in a column were placed just above the slabs (see Figs. 1 and 3).

It is worthwhile to note that as shown in Fig. 1 the upper part of columns has continuous longitudinal bars whereas the lower part of columns has lap splices. Thus this study made specimens representing the upper part and lower part of columns (see Fig. 2). It was assumed that the inflection point was located at the mid-height of the column during earthquakes.

Fig. 3 shows the reinforcement details and dimensions of the 2/3 scale column test specimens. Table 1 describes the characteristics of the specimens. All reinforcements were scaled by 2/3 for test specimens. A total of eight specimens were made (upper and lower part (2) of interior and exterior columns in OMRCF and IMRCF (2)). Lap splice length (350 mm) was also simply scaled by 2/3 of the original length (525 mm). No attempt was made to re-calculate lap splice length for scaled reinforcement. Rebar D13 (12.7 mm diameter) and D6 (6.35 mm diameter) were used for longitudinal and transverse tie reinforcement to represent 2/3 of D19 and D10 in the columns of model frames.

The dimension of column base is shown in Fig. 3. The longitudinal reinforcement of column specimens was anchored to the column base satisfying development length required by ACI 318-02 (chapter 12). In order to fix the specimen to the strong floor, four high strength bolts having a diameter of 70 mm were installed (see Fig. 4(a)). All bolts are fully tightened to provide specimens with fixed base conditions. In column base, sufficient closed type stirrups using reinforcement of D13 (13 mm diameter) were placed to resist the forces transferred from the specimen. No cracks were detected in the column base after test (see Fig. 4(a)).

3.3. Material tests

Based on concrete trial mixes from various recipes for attaining the 28-day target strength (f'_c) of 23.5 MPa, a design mix was determined. The maximum size of aggregate for 2/3 scale model specimens was 25 mm. Cylinder tests were performed. Each concrete cylinder was 200 mm in height and 100 mm in diameter. Cylinder test results are given in Table 2.

Longitudinal and transverse reinforcement in the column specimens (2/3 scale) were D13 (13 mm diameter) and D6 (6 mm diameter), respectively. The results of material tests are given in Table 3.

3.4. Loading and measurements

All eight-column specimens were laterally loaded at the level of 1000 mm above the base (mid-height of a column) (see Fig. 4). It was assumed that the inflection point of a column is located at mid-height of the column.

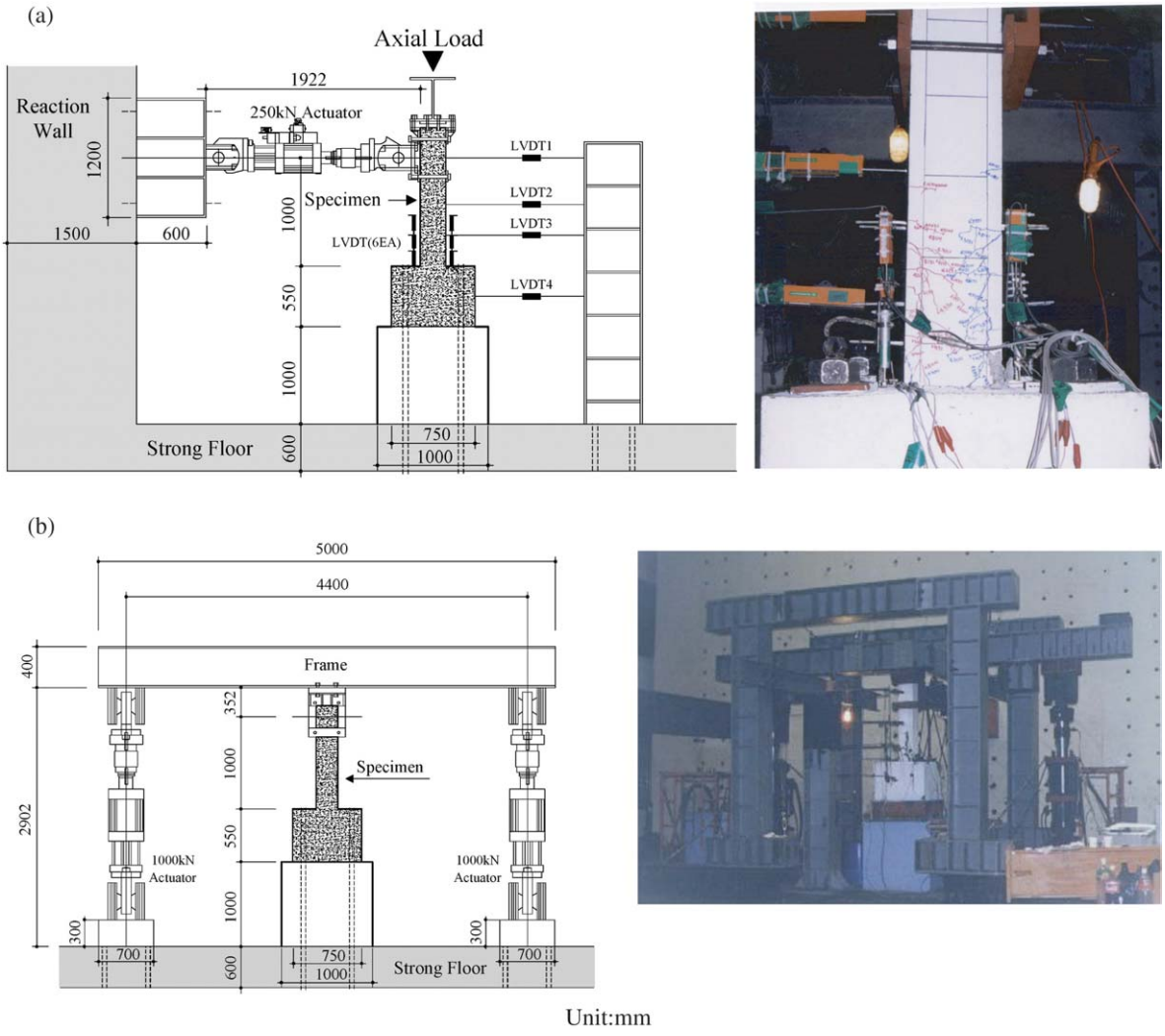

Fig. 4. Test setting.

Table 1
Characteristics of the column specimens

	Location		Specimen name	Loading plan	Lap splice
OMRCF (IMRCF)	Interior column	Lower part	OIL (IIL)	Constant axial load ($P = 0.28$)	○
		Upper part	OIN (IIN)		×
	Exterior column	Lower part	OEL (IEL)	Varying axial load ($P = 1.83V + 17.1$)	○
		Upper part	OEN (IEN)		×
O I L (1) (2) (3)		(1): OMRCF (O), IMRCF (I) ○: having lap splices (2): Interior (I), Exterior (E) ×: not having lap splices (3): with lap splice (L), without lap splice (N)			

Quasi-static reversed cyclic loading (displacement controlled) was applied. Two cycles were applied for each loading amplitude. The loading history is shown in Fig. 5. Since fluctuation of axial loads in the exterior columns was more significant than in the interior columns, varying axial loading was applied to the exterior column specimens, whereas a constant axial load was applied to the interior column specimens. Larger axial loads were applied to interior columns due to a larger tributary area.

Axial loads were calculated by frame analysis using SAP 2000 commercial software [5] without considering load factors. Since specimens were scaled by 2/3, calculated

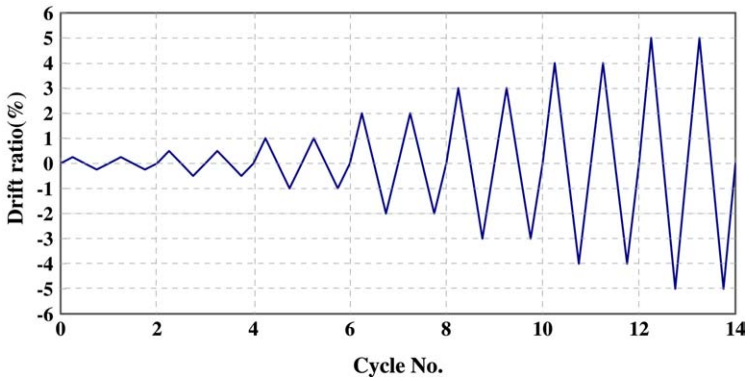

Fig. 5. Loading history.

Table 2
Concrete properties of the specimens

Design strength (MPa)	28 day strength (MPa)	Strain at ultimate strength, ε_{co}	Young's modulus (MPa)
23.5	24.6	0.003	23,438

Table 3
Reinforcing steel properties

Bar	Yielding strength (MPa)	Yielding strain ($\times 10^{-6}$)	Ultimate strength (MPa)	Young's modulus (MPa)
D6	374	2206	598	176,520
D13	397	2035	594	194,956

force for original frame members should be scaled by 4/9 for the scaled model. Interior column specimens (OIL, OIN, IIL, IIN) were tested with a constant axial load of 333.4 kN ($0.28\,A_g\,f_c'$; A_g is the gross sectional area of a column). For exterior column specimens, varying axial loads (P (axial force) $= 1.83V$ (lateral force) $+ P_g$) were applied. P_g is gravity axial load, which is 167.6 kN, and V is lateral shear force acting on the column. This relationship was also obtained using SAP 2000 under first mode lateral force profile. The range of varying axial loads for exterior column specimens is $0.07 \sim 0.20 A_g\,f_c'$.

As shown in Fig. 4, one actuator was installed to control lateral forces and two actuators were used to control axial forces. Three pairs of linear transducers were placed at the column faces to capture column curvatures (see Fig. 4(a)). However, curvature results were not included in this paper. One LVDT was also placed to measure a lateral displacement of the stub of column specimens. Since it was observed that slip between the stub and strong floor is negligible during the test, recorded displacement of column specimens was not modified. This was due to tightened bolts passing through stubs of specimens. Curvature of stubs was not measured since it was assumed that tightened bolts made a rigid base condition. Four linear transducers were installed to measure the lateral displacements of specimens.

4. Test results and observation

4.1. Observations

Within a drift ratio of ±1%, the first flexural crack was observed in all specimens. The lateral force causing the first crack in all specimens was about 25 kN. At a drift ratio of ±3%, the concrete cover started spalling at the column ends. It is noted that drift ratio was defined as a measured lateral displacement divided by the height of specimens.

In the exterior column specimens having lap splices (OEL, IEL), spalling and cracks (vertical and horizontal) were more prominent when applied lateral loading was in the positive direction (the direction in which axial load increases). As mentioned earlier, varying axial loads ($P = 1.83V + 167.6$ (kN)) were applied to exterior column specimens. Moreover, many vertical cracks in the region of lap splices were observed. Flexural cracks were relatively uniformly distributed in the plastic hinging region of the specimens.

In the final stage of the test, all column specimens failed due to buckling of the longitudinal bars and crushing of the concrete.

4.2. Hysteretic performance

Hysteretic curves for the OMRCF and IMRCF columns are presented in Figs. 6 and 7, respectively. Fig. 6(a), (b) and (c), (d) shows the hysteretic curves for the interior specimens OIL and OIN, and for the exterior column specimens OEL and OEN of the OMRCF. Fig. 7(a), (b) and (c), (d) show the curves for the interior specimens IIL and IIN, and for the exterior column specimens IEL and IEN of the IMRCF. All column specimens behaved almost elastically until a drift ratio of ±0.3%.

According to Fig. 6(a) and (b), strength of specimens OIN and OIL was similar irrespective of the existence of lap splices. However, specimen OIN exhibited greater deformation capacity than the OIL specimen having lap splices. In the IMRCF interior column specimens, IIN and

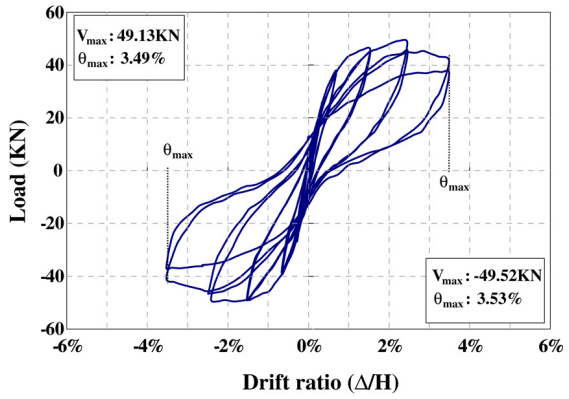

(a) OIL.

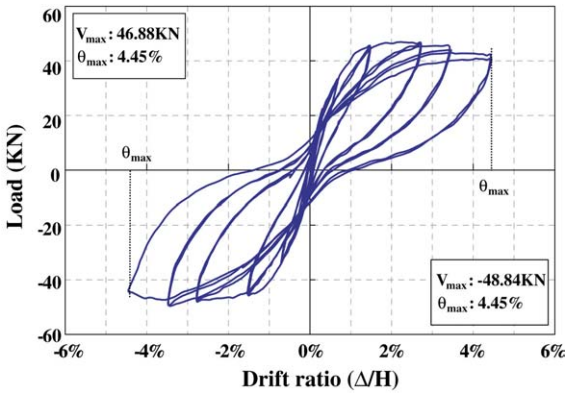

(b) OIN.

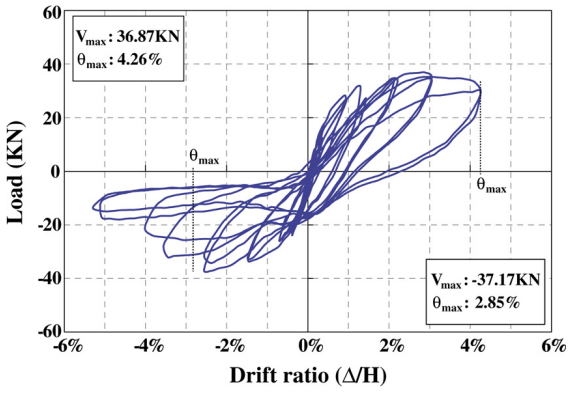

(c) OEL.

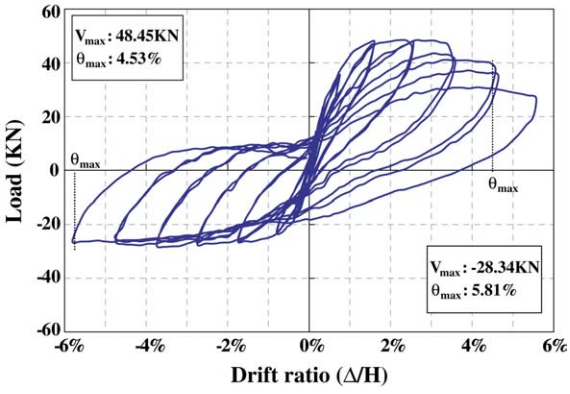

(d) OEN.

Fig. 6. Hysteretic curves of the OMRCF columns.

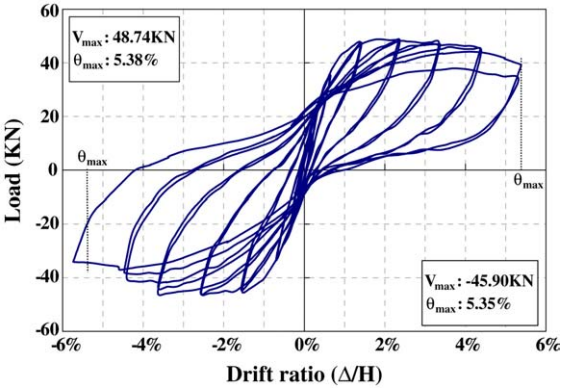

(a) IIL.

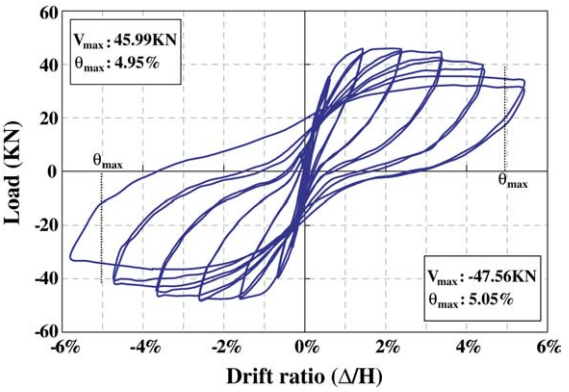

(b) IIN.

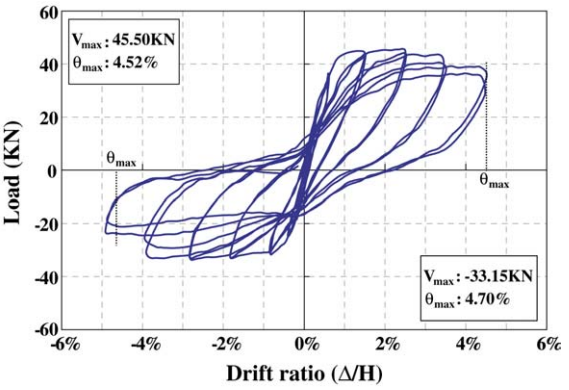

(c) IEL.

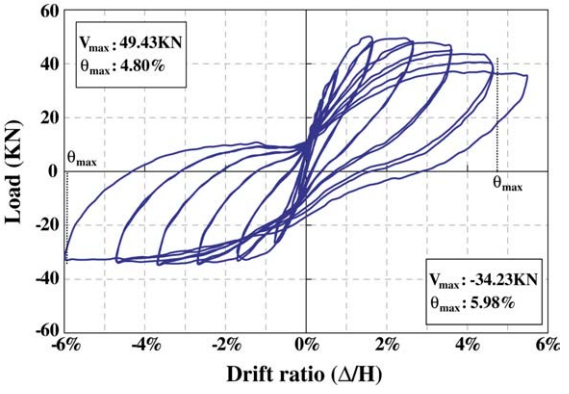

(d) IEN.

Fig. 7. Hysteretic curves of the IMRCF columns.

IIL, (Fig. 7(a) and (b)), no discernible difference could be found in either strength or deformation capacity.

The strength of all the OMRCF and IMRCF interior column specimens (OIN, OIL, IIN, IIL) was similar, whereas OMRCF interior columns had inferior deformation capacities to the IMRCF interior columns. Moreover, pinching was detected more prominently in OMRCF specimens. Strength drops in the second cycle were, however, similar between the OMRCF interior column specimens and their corresponding IMRCF specimens.

In interior column specimens, IMRCF has a more stable and fuller hysteretic curve than OMRCF. In particular, the improvement was more prominent when columns had lap splices (compare Figs. 6(a) and 7(a)). The better hysteretic behavior in interior columns of IMRCF was attributed to narrower spacing of transverse reinforcement in the plastic hinging region of the column.

Fig. 8(a) shows the envelope curves extracted from the hysteretic curves of the interior column specimens. According to this figure, the IMRCF specimens had fuller envelope curves than the OMRCF specimens. Thus, it is expected that interior column specimens of IMRCF exhibited better seismic behavior than those of OMRCF. Since larger axial force was applied to the interior specimens due to a larger tributary area of gravity loads, narrower spacing of transverse reinforcement in the plastic hinge region improved the seismic behavior of the columns significantly.

Figs. 6(c) and (d), and 7(c) and (d) show hysteretic behaviors of the exterior column specimens of the OMRCF (OEL, OEN) and IMRCF (IEL, IEN), respectively. In these figures, the positive loading direction was the direction in which the axial load increases.

The hysteretic behaviors of the exterior OMRCF and IMRCF column specimens were relatively similar between the OMRCF specimens and corresponding IMRCF specimens (OEN versus IEN, and OEL versus IEL). However, the strength drop of specimen OEL in the second cycle was greater than that of specimen IEL. The specimens having lap splices showed inferior deformation capacities compared to the specimens without lap splices (OEL versus OEN, and IEL versus IEN). Unlike interior columns, hysteretic behavior was not significantly improved by narrower spacing of lateral reinforcement (OEL versus IEL, and OEN versus IEN). Fig. 8(b) shows the envelope curves. From this figure, the specimens having lap splices also had narrower envelope curve. Also, this figure shows that the envelope curves of the exterior column specimens of OMRCF and IMRCF are quite similar (OEN versus IEN, and OEL versus IEL). However, more strength drop in specimen OEL was observed than that in IEL in the negative loading direction. In exterior column specimens, lateral reinforcement spacing does not affect seismic behavior as much as in the interior column specimens. However, it was observed that seismic behavior in exterior column specimens became poor when they had lap splices.

4.3. Maximum strength

Table 4 shows the ratio of actual maximum strength M_{max} obtained from experimental tests to the calculated strength (M_{ACI}). Actual maximum strength M_{max} is calculated by maximum shear force times the height of the column specimen ($M_{max} = V_{max} \times \mathbf{1}m(h)$). Fig. 9 shows P–M interaction curves of column specimens. This figure also includes the actual moment strength (M_{max}) of column specimens. All nominal strength (M_{ACI}) in this study was calculated using material strength obtained from material tests. According to Fig. 9 and Table 4(7), all OMRCF and IMRCF column specimens have strength larger than calculated nominal strength.

In exterior column specimens, moment capacities (M_{max}) in the positive loading direction were greater than those in the negative loading direction. Since axial loads in the test are not large, strength of column specimens is below the balanced failure point in P–M interaction curve. Thus, in exterior column specimens, moment strength increases as axial force is larger (positive lateral loading direction).

In the P–M interaction curve (Fig. 9), calculated moment strength (M_{ACI}) of exterior column specimens in the positive loading direction is larger than that in the negative loading direction as well. In those specimens with relatively low axial loads, the ratio of maximum strength (M_{max}) to calculated strength (M_{ACI}) was almost the same as that of the interior column specimens.

It is worthwhile to note that all column specimens were designed according to the minimum design and detail requirements in ACI 318-02. Since all specimens in this study were governed by flexure rather than shear (see Table 4(10)), different results can be obtained for columns governed by shear.

4.4. Deformation capacity

In this study the maximum drift ratio ($\theta_{max} = \Delta_{max}/h$) was used to determine the drift capacities, where Δ_{max} is the maximum drift and h is the height of column specimens. The maximum drift was obtained when the lateral strength of the specimen was reduced by 20% of maximum strength. Table 4 and Fig. 10 show the maximum drift ratios of the specimens.

Table 4 shows that the drift capacities (θ_{max}) of OMRCF and IMRCF exceeded 3.0% and 4.5%, respectively. Specimen IEN had the largest drift capacity (5.98%) in the negative loading direction, whereas specimen OEL had the least drift capacity (3.00%) in the negative loading direction.

Among the interior column specimens that resisted a larger constant axial load throughout the test, the IMRCF columns had greater drift capacity. This is due to the narrower spacing of transverse reinforcement in the plastic hinging region. It should be noted that the drift capacity of the specimen IIL having lap splices was even greater than that of OIN without lap splices. Moreover, the difference

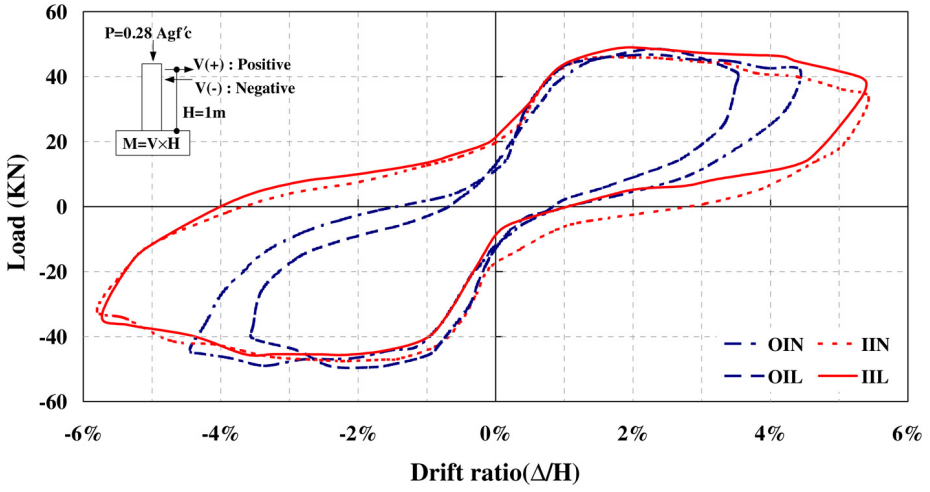

(a) Interior columns.

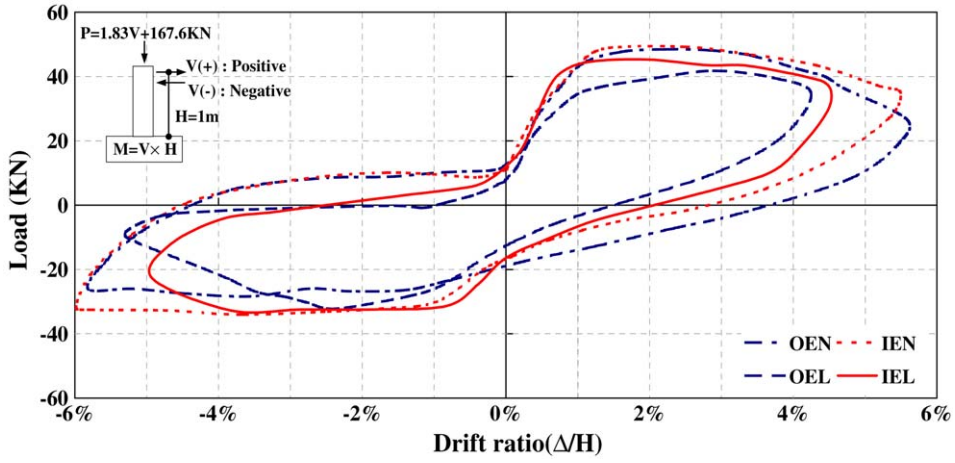

(b) Exterior columns.

Fig. 8. Envelope curves.

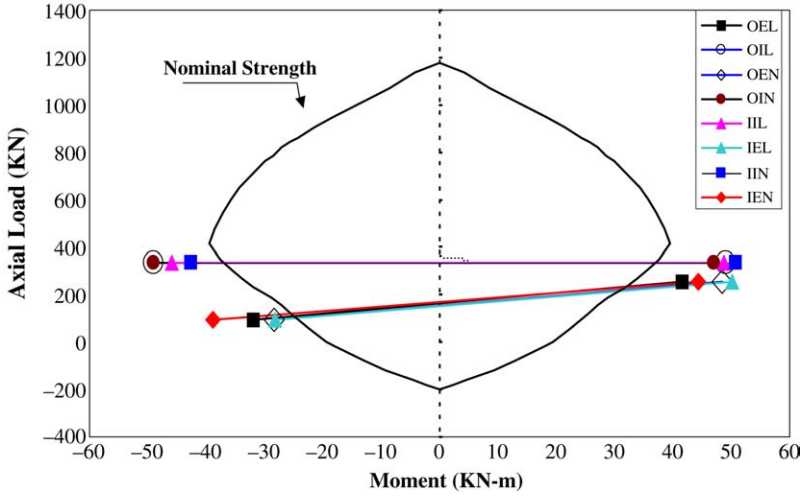

Fig. 9. Maximum strength.

Table 4
Test result of specimens

Specimen			$\frac{P_u}{A_g f_c'}$ (1)	V_{max} (2)	Δ_{max} (3)	μ_Δ (4)	θ_u (5)	M_{ACI} (6)	$\frac{M_{max}}{M_{ACI}}$ (7)	V_{ACI} (8)	V_P (9)	$\frac{V_P}{V_{ACI}}$ (10)
OMRCF	OIL	+	0.28	49.1	34.9	4.26	3.49	36.8	1.33	74.3	37.9	0.51
		−		49.5	35.3	4.46	3.53	36.8	1.33	74.3	37.9	0.51
	OIN	+		46.9	44.5	4.41	4.45	36.8	1.28	74.3	37.9	0.51
		−		48.8	44.5	4.39	4.35	36.8	1.33	74.3	37.9	0.51
	OEL	+	0.2	36.9	42.6	4.34	4.26	33.3	1.25	69.6	32.6	0.47
		−	0.07	37.2	28.5	3.02	3.01	25.5	1.25	63.4	26.0	0.41
	OEN	+	0.2	48.5	45.3	4.59	4.53	33.4	1.45	69.6	32.6	0.47
		−	0.07	28.3	58.1	6.05	5.81	25.5	1.11	63.4	26.0	0.41
IMRCF	IIL	+	0.28	48.7	53.8	6.02	5.38	38.8	1.28	9.83	3.88	0.39
		−		45.9	53.5	5.57	5.35	38.8	1.21	9.83	3.88	0.39
	IIN	+		46.0	49.5	6.10	4.95	38.8	1.34	9.83	3.88	0.39
		−		47.6	50.5	6.01	5.05	38.8	1.22	9.83	3.88	0.39
	IEL	+	0.2	45.5	45.2	5.82	4.52	33.0	1.55	9.36	3.30	0.35
		−	0.07	33.2	47.0	5.90	4.70	26.2	1.10	8.72	2.62	0.30
	IEN	+	0.2	49.4	48.0	5.9	4.80	33.0	1.37	9.36	3.30	0.35
		−	0.07	34.2	59.8	6.27	5.98	26.2	1.31	8.72	2.62	0.30

(2) = maximum shear force (kN), (3) = maximum displacement (mm), (4) = displacement ductility (= Δ_{max}/Δ_y), where Δ_y is yield displacemet, (5) = maximum drift angle (%), (6) = moment capacity calculated using ACI 318-02 procedures (kN m), (7) = ratio of the maximum moment capacity, $M_{max}(V_{max} \times h)$ to M_{ACI} (h: height of specimen (m)), (8) = nominal shear strength according to ACI 318-02 (kN), (9) = shear force corresponding to M_{ACI} or $2M_{ACI}/l$, where l = the column clear height (kN), (10) = ratio of V_P to V_{ACI}.

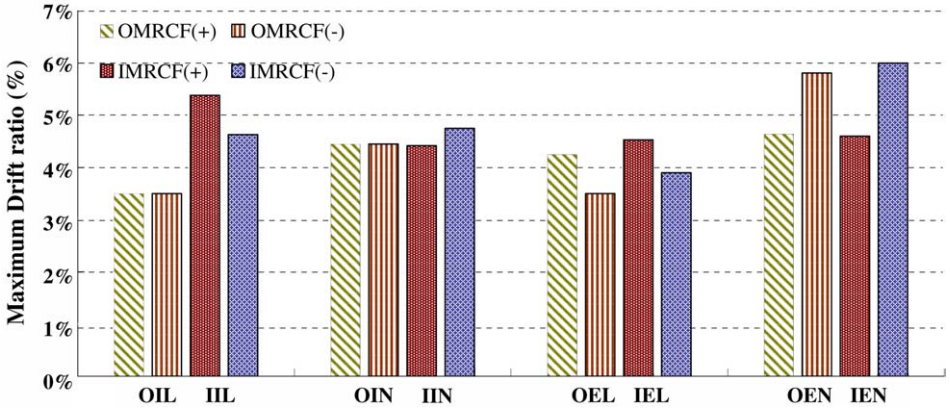

Fig. 10. Drift capacity (%).

between drift capacities of specimens OIL and IIL was greater than that of specimens OIN and IIN. Thus, spacing of transverse reinforcement in the plastic hinging region affects the drift capacity of the interior columns significantly. This was more prominent when the specimen had lap splices. It is noted that larger gravity load ($0.28A_g f_c'$) was applied to interior column specimens. Also, in interior column specimens of OMRCF, the existence of lap splices in the column specimen prominently influences the drift capacity. In contrast, the existence of lap splices did not affect drift capacities of IMRCF column specimens.

In the exterior column specimens that resisted varying axial loads during the test, the existence of lap splices also affected drift capacities. Specimens IEL and OEL having lap splices had smaller drift capacities. The difference between drift capacities of the exterior columns of the OMRCF and IMRCF was small compared to that between the interior columns of the OMRCF and IMRCF. Thus, in the exterior columns, the spacing of transverse reinforcement was not influential. It is noted that this study considered a three-story building, in which axial forces in columns are small compared with those in high-rise buildings. When axial forces in columns become large, the spacing of transverse reinforcement may be influential even on the behavior of exterior columns.

This study also calculated the displacement ductility of each specimen, which is shown in Table 4. Yield drift (Δ_y or θ_y) was obtained from a bilinear representation of force (V) versus drift ratio (Δ or θ). Secant stiffness was used to connect the origin to the point of $0.75V_{max}$. The

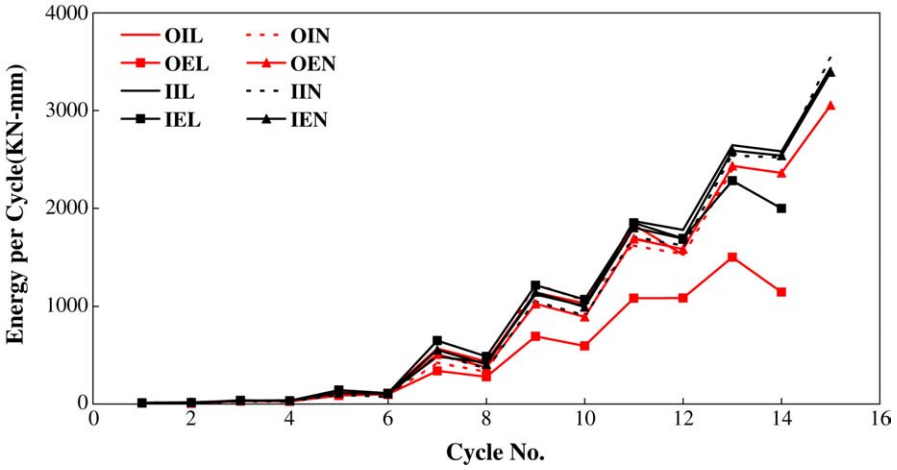

Fig. 11. Energy dissipation.

maximum drift ($\Delta_{max}, \theta_{max}$) was approximated as the drift ratio corresponding to the strength deteriorated by 20% of V_{max} (0.8 times V_{max}). As shown in Table 4, all specimens have a ductility capacity exceeding 3.0. The IMRCF exterior column specimen without lap splices (IEN) has the largest ductility capacity (6.27) in the negative loading direction which has the least axial loading condition ($\frac{P_u}{A_g f'_c} = 0.07$). In contrast, the OMRCF exterior column specimen with lap splices (OEL) has the smallest ductility capacity (3.02) in the negative loading direction. Specimen IEL has a ductility capacity of 5.90 in the negative loading direction. Thus the effect of lateral reinforcement spacing on displacement and ductility capacity becomes important to all interior column specimens, and exterior specimens having lap splices.

4.5. Energy dissipation

Fig. 11 shows the amount of energy dissipated in each loading cycle. According to this figure, all specimens dissipated a similar amount of energy until cycle 6 (1% drift ratio). Beyond that cycle, every specimen dissipated a different amount of energy.

Specimens IIN, IIL, and IEN dissipated similar amounts of energy until failure. They have larger energy dissipation capacity than other specimens. Specimens OEN, OIN, and IEL dissipated similar amounts of energy until cycle 13 (5%). Since specimen OIL failed in an earlier loading stage (cycle 11), the amount of energy of specimen OIL is smaller than specimens OEN, OIN and IEL. Specimen OEL has the least amount of energy dissipation capacity among the specimens.

5. Conclusions

This study investigates the seismic behaviors of columns in OMRCF and IMRCF. For this purpose eight specimens were modeled and tested. The specimens were designed and reinforced in compliance with the ACI 318-02 for OMRCF and IMRCF. It should be noted that all specimens were governed by flexure rather than shear. Thus, different results may be obtained for columns governed by shear. The conclusions of this study are as follows:

(1) The strength of all OMRCF and IMRCF column specimens exceeded the strength calculated with the code formula (ACI 318-02). Thus, the OMRCF and IMRCF columns had satisfactory strength irrespective of the existence of the lap splices and the transverse reinforcement spacing in the plastic hinging region.

(2) The IMRCF interior column specimens had superior drift capacities compared to the OMRCF column specimens. Existence of lap splices influenced drift capacities of the OMRCF columns. However, the effect of lap splice in the IMRCF columns was not as large as that in the OMRCF specimens. This is attributed to the narrower transverse reinforcement spacing in the plastic hinging region of the IMRCF.

(3) In the exterior column specimens, no discernible differences in the hysteretic behaviors were found between OMRCF and IMRCF column specimens. The specimens having lap splices showed inferior hysteretic behavior to the corresponding specimens without lap splices. Since smaller axial force was applied to the exterior column specimens, the effect of transverse reinforcement spacing seems to be less influential than interior columns. However, it is noted that the effect of transverse reinforcement spacing becomes important to exterior specimen having lap splices, particularly in the negative loading direction.

(4) IMRCF interior column specimens had more stable and fuller hysteretic curves than OMRCF interior column specimens. In OMRCF interior column specimens, existence of lap splices changed the shape of hysteretic curve significantly. However, in IMRCF interior column specimens, the change due to lap splices was not noticeable.

(5) In exterior column specimens of OMRCF and IMRCF, hysteretic curves became narrower when they had lap splices. However, the hysteretic curves of OMRCF exterior columns are similar to those of corresponding IMRCF exterior columns.
(6) According to the test results, the OMRCF and IMRCF column specimens had drift capacities greater than 3.0% and 4.5%, respectively. Ductility capacity of those specimens exceeded 3.01 and 4.53, respectively.

Acknowledgement

The support of Hanyang University is greatly acknowledged.

References

[1] American Concrete Institute. Building code requirements for reinforced concrete, ACI 318-95, 99, 02, Detroit, Michigan, 1995, 1999, 2002.
[2] Uniform Building Code (UBC). International conference on building officials. 1997.
[3] Building Seismic Safety Council. NEHRP recommended provisions for the development of seismic regulation for new buildings, Part 1 and 2, provisions and commentary, Washington, DC: FEMA; 1994, 1997.
[4] Portland Cement Association. Notes on ACI 318-99, 02 building code requirements for structural concrete, Skokie, Illinois, 1999, 2002.
[5] Computers and Structures Inc. SAP2000, 1997.
[6] Han SW, Kwon OS, Lee L-H, Foutch DA. Seismic performance evaluation of ordinary moment resisting concrete frames. SRS No. 633, Urbana, Illinois; 2002 November.
[7] Han SW, Kwon OS, Lee L-H. Evaluation of the seismic performance of a three-story ordinary moment resisting concrete frame. Earthquake engineering and structural dynamics, vol. 33. Wiely and Sons; 2004. p. 669–85.
[8] BOCA, ICBO, SBCCI. International Building Code. 2000.
[9] Lee H-S, Woo S-W. Effect of masonry infills on seismic performance of a 3-storey RC frame with non-seismic detailing. Earthquake engineering and structural dynamics, vol. 31. Wiely and Sons; 2002. p. 353–78.
[10] Aycardi LE, Mander JB, Reinhorn AM. Seismic resistance of reinforced concrete frame structures designed only for gravity loads: experimental performance of subassemblages. Structural Journal American Concrete Institute 1994;91:552–63.
[11] Lynn A, Moehle J, Mahin SA, Holmes WT. Seismic evaluation of existing RC building columns. Earthquake Spectra 1996;12(4): 715–39.

Sang Whan Han. Associate Professor, Dept. of Architectural Eng., Hanyang Univ., Seoul 133-791, Korea. Ph.D. (1994), University of Illinois at Urbana-Champaign, Professional Engineer (US, Korea).

N.Y. Jee. Professor, Dept. of Architectural Eng., Hanyang Univ., Seoul 133-791, Korea. Ph.D. (1992), Tokyo National University.